# Stable N-bridged diiron (IV) phthalocyanine cation radical complexes: synthesis and properties†

**Pavel Afanasiev,[a] Denis Bouchu,[b] Evgeny V. Kudrik,[a] Jean-Marc M. Millet[a] and Alexander B. Sorokin*[a]**

***Received 5th August 2009, Accepted 16th September 2009***
***First published as an Advance Article on the web 7th October 2009***
**DOI: 10.1039/b916047g**

Oxidation of N-bridged diiron tetra-*tert*-butylphthalocyanine $(FePc^{t}Bu)_2N$ with $^{t}BuOOH$ in halogenated solvents afforded μ-nitrido diiron (IV) phthalocyanine cation radical complexes, $(X)PcFe^{IV}–N–Fe^{IV}Pc^{+\bullet}(X)$ (X = Cl, Br), as evidenced by UV-vis, electron paramagnetic resonance (EPR), electrospray ionization mass spectrometry (ESI-MS), Mössbauer, X-ray absorption near edge structure (XANES) and extended X-ray absorption fine structure (EXAFS) data. Continuous introduction ESI-MS showed the initial formation of the *t*-butylperoxo diiron complex $^{t}BuOO$-$(FePc^{t}Bu)_2N$ followed by intermediate formation of a monohalogenated adduct which gave the dihalogenated complex as final stable product. Fe K-edge EXAFS analysis of $(X)PcFe^{IV}–N–Fe^{IV}Pc^{+\bullet}(X)$ showed bridging N atom at a distance of 1.69(1) Å. The distance between two equivalent hexacoordinated in-plane iron (IV) centers is 3.39(1) Å. Fe–X bond lengths are 2.33 and 2.54 Å for X = Cl and Br, respectively. The use of $(Cl)PcFe^{IV}–N–Fe^{IV}Pc^{+\bullet}(Cl)$ for the catalytic oxidation of organic substrates has been shown for the first time.

## Introduction

Active sites of many enzymes involved in biological oxidation contain binuclear O-bridged diiron structures in non-heme environments.[1] The fascinating properties of these enzymes, such as their ability to carry out difficult oxidations (*e. g.* oxidation of methane) have stimulated numerous studies with the objective of developing biomimetic catalytic systems.[2] Significant progress has been achieved with structural and spectroscopic modelling to allow the better understanding of the mechanisms of biological oxidation. However, functional models capable of oxidizing strong C–H bonds are still rare.

Recently, we proposed the use of binuclear diiron complexes on a phthalocyanine platform as catalysts for oxidation.[3] The use of a nitrogen atom bridging two iron sites in a macrocyclic environment resulted in remarkable catalytic properties, including the mild oxidation of methane,[3a] benzene[3b] and alkyl aromatic compounds.[3d] Before our work, N-bridged binuclear complexes have never been evoked as catalysts for oxidation, although a number of such complexes involving phthalocyanine,[4] porphyrin[5] and mixed ligands systems[6] have been described and recently reviewed by Ercolani *et al.*[7] The good catalytic properties of N-bridged structures might be due to the stabilization of high oxidation states of iron by the μ-nitrido ligand. Indeed, mononuclear $LFe^{V}\equiv N$[8] and even $LFe^{VI}\equiv N$[9] species have been described. A limited number of N-bridged binuclear phthalocyanine complexes containing five-coordinated Fe(IV),[4a,6b,6c,6i,10] and six-coordinated Fe(IV)[4b,4c,6b,6d,6f,6h,10c] centers has been described in literature. Taking into account the unusual catalytic properties of N-bridged diiron complexes in oxidations that probably involve high-valent diiron intermediates,[3] the demand for the preparation and characterization of stable high-valent diiron structures is high.

Formally, symmetrical N-bridged diiron complexes are mixed valence $Fe^{III}–Fe^{IV}$ species, but spectroscopic studies showed two equivalent iron centers with the intermediate +3.5 oxidation state due to efficient electron exchange.[7] The neutral $PcFe^{+3.5}–N–Fe^{+3.5}Pc$ species can be oxidized to $[PcFe^{IV}–N–Fe^{IV}Pc]^{+}X^{-}$ complexes using one electron oxidants, for example the ferrocenium cation.[4b] The single doublet in the Mössbauer spectrum with a negative value of isomeric shift ($\delta$ = –0.10 mm $s^{-1}$) and the absence of EPR signals indicated metal-centered oxidation to form the $[PcFe^{IV}–N–Fe^{IV}Pc]^{+}$ structure. A two electron electrochemical oxidation of $PcFe^{+3.5}–N–Fe^{+3.5}Pc$ in DMF/LiBr furnished $(Br)PcFe^{IV}–N–Fe^{IV}Pc(Br)$.[11] The X-ray sructural determination showed two six coordinated iron centers with short Fe–N distances (1.639 Å) and a linear Br–Fe–N–Fe–Br structure. Two phthalocyanine rings are staggered by an angle of 39°, with an in-plane location of the Fe atoms. The second diiron (IV) complex that contains halogen ligands was described by Murray *et al.*[4c] Oxidation of $PcFe^{+3.5}–N–Fe^{+3.5}Pc$ by bromine, trifluoroacetic or nitric acid afforded red-brown complexes. The EPR spectra showed a singlet signal with g = 2.0, typical for an organic radical. The absorption bands at 1350 and 1459 $cm^{-1}$ in the IR spectra were also indicative of the presence of the phthalocyanine cation radical. Negative values of isomeric shift in the Mössbauer spectra were consistent with the Fe(IV) oxidation state. The authors propose that the $[(X)PcFe^{IV}–N–Fe^{IV}Pc(X)]^{+}X^{-}$ (X = $Br^{-}$, $CF_3CO_2^{-}$, $NO_3^{-}$) formulation[4c] can be considered as result of three electron oxidation of the starting $PcFe^{+3.5}–N–Fe^{+3.5}Pc$ complex. To date, only two bromine containing N-bridged diiron complexes have been prepared.

[a]*Institut de Recherches sur la Catalyse et l'Environnement de Lyon (IRCELYON), UMR 5256, CNRS-Université Lyon 1, 2, av. A. Einstein, 69626, Villeurbanne Cedex, France. E-mail: alexander.sorokin@ircelyon.univ-lyon1.fr; Fax: +33 472445399; Tel: +33 472445337*
[b]*Université Lyon 1, UMR 5246, Centre Commun de Spectrométrie de Masse, 43 bd du 11 novembre 1918, 69622, Villeurbanne cadex, France*
† Work first presented at the 10th FIGIPAS Meeting in Inorganic Chemistry, Palermo, July 1–4, 2009

 

In the course of our studies, we found a novel method for the preparation of N-bridged high valent diiron complexes which provide access not only to bromine but also to chlorine containing complexes. The N-bridged diiron tetra-*tert*-butylphthalocyanine complex (Fig. 1, **1**) was used in this study to access species soluble in common organic solvents.

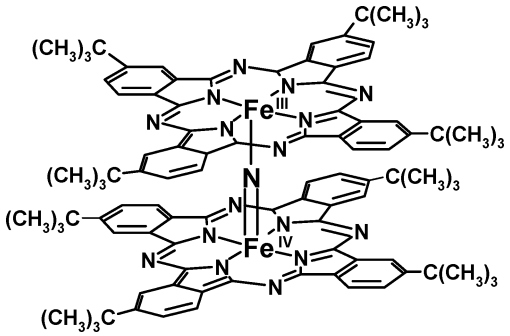

**Fig. 1** Structure of N-bridged diiron tetra-*tert*-butylphthalocyanine, **1**.

Here we report on the preparation of two stable complexes with $Cl^-$ and $Br^-$ ligands and their characterization by UV-vis, electrospray ionization mass spectrometry (ESI-MS), Mössbauer, electron paramagnetic resonance (EPR), X-ray absorption near edge structure (XANES) and extended X-ray absorption fine structure (EXAFS) techniques, as well as their first use as catalysts for oxidation.

## Results

### Reaction of 1 with $^t$BuOOH in $CH_2Cl_2$

The addition of $^t$BuOOH to a solution of **1** in $CH_2Cl_2$ resulted in a two step reaction, as indicated by UV-vis spectroscopy (Fig. 2). In the first fast reaction, the intensity of the Q band at 641 nm decreased and two new broad bands centered at 536 and 677 nm appeared. The positions and broad character of these new bands are consistent with the formation of the phthalocyanine cation radical.[12] Metal-centered one electron oxidation usually results in relatively small UV-vis spectral changes. For example, upon oxidation of $PcFe^{+3.5}$–N–$Fe^{+3.5}Pc$ to $[PcFe^{IV}$–N–$Fe^{IV}Pc]^+$ by the ferrocenium cation, the maximum of the Q-band batochromically shifted from 625 to 642 nm without formation of new bands. In the second slower step, small but distinctive changes resulted in the blue shifting of the band at 640 nm to 629 nm with a decrease of the intensity. Interestingly, similar features were observed when $CH_2Br_2$ was used instead of $CH_2Cl_2$.

In order to identify novel species, the reaction of **1** with $^t$BuOOH in $CH_2Cl_2$ was studied by continuous introduction positive electrospray ionization mass spectrometry (ESI-MS). In $CH_2Cl_2$ solution **1** exhibits one prominent signal of the molecular peak $[M]^+$ at $m/z = 1599$, with a corresponding isotopic pattern of the molecular cluster (Fig. 3a).

Immediately after the addition of $^t$BuOOH, a new signal at $m/z = 1688$ was detected, corresponding to $[M+89]^+$, indicating the coordination of $^t$BuOO$^-$ to **1**, with retention of its binuclear structure (Fig. 3b). The mass spectrum recorded 4.6 min after the addition of $^t$BuOOH showed an intense signal at $m/z = 1634.4$ along with the molecular peak of **1** to its left (Fig. 3c). The $m/z$ value and isotopic distribution of this signal indicated the formation of the adduct of **1** with one chlorine atom (**2**). The formation of **2** can be explained by the oxidative dechlorination of $CH_2Cl_2$, which can be performed by the active species formed from the **1**+OO$^t$Bu complex. Then, the intensities of the signals of **1** and **2** decreased and a novel signal centered at $m/z = 1670.5$ appeared (Fig. 3d). The isotopic pattern of this signal fitted to the **1**+2Cl formulation (complex **3**).

Taking into account that mass spectrometry alone does not provide a definite structural assignment, we prepared complexes **3** and **4** in the solid state and further characterized them by

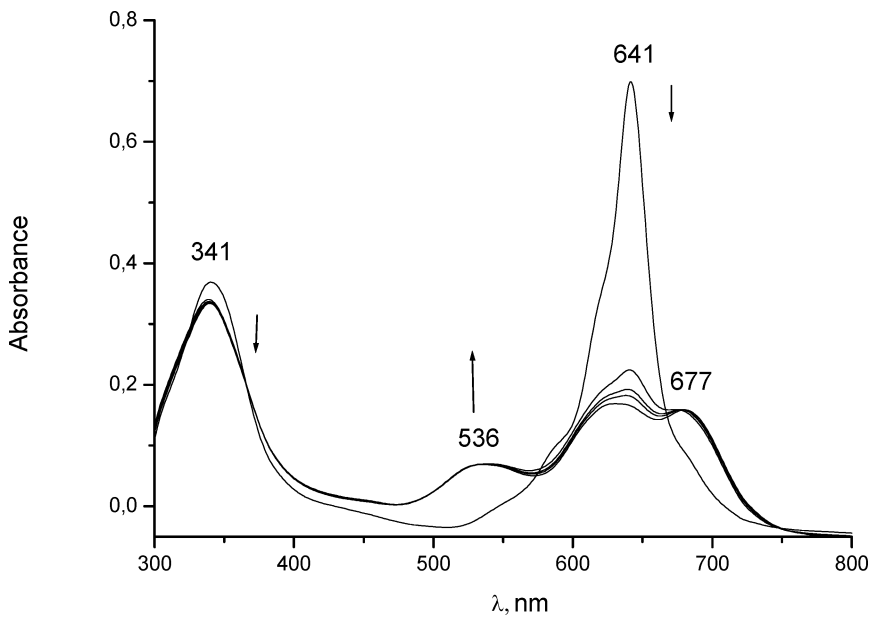


**Fig. 2** Spectral changes observed in the reaction of **1** with $^t$BuOOH. Experimental conditions: $CH_2Cl_2$, $[\mathbf{1}] = 2.0 \times 10^{-6}$ M, [$^t$BuOOH] = 0.015 M, 25 °C, spectra recorded after 3 min intervals.

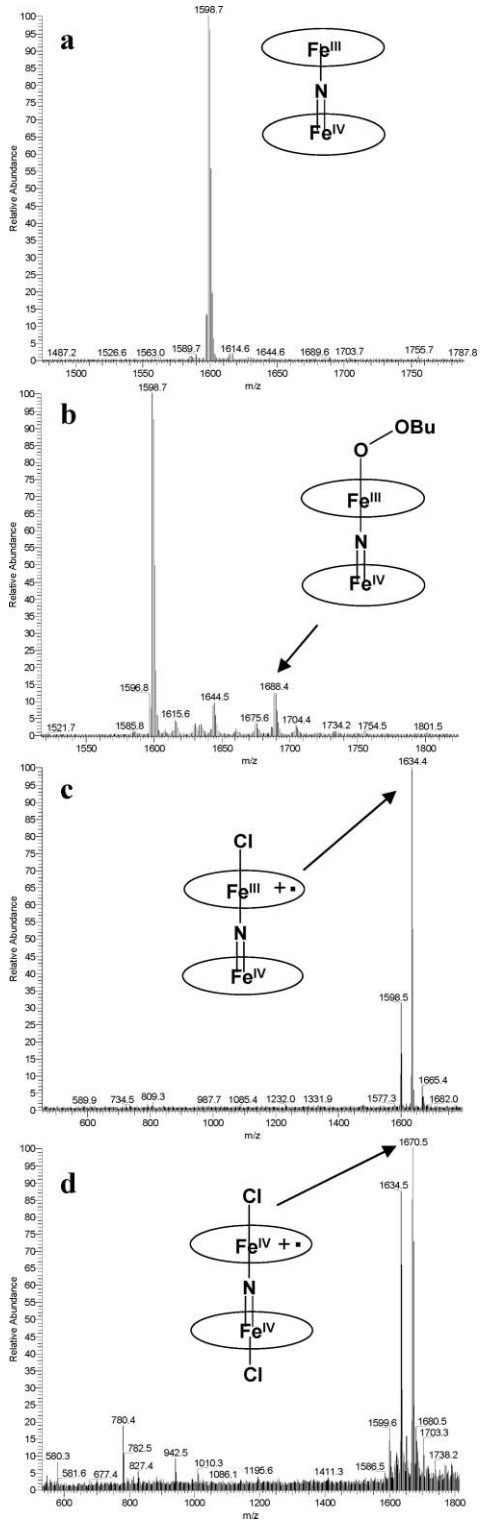


**Fig. 3** ESI-MS spectra recorded in the course of the reaction of **1** with $^{t}$BuOOH in $CH_2Cl_2$. Experimental conditions: [**1**] = ~$1.0 \times 10^{-6}$ M, [$^{t}$BuOOH] = ~0.01 M, 25 °C. (a) Initial complex 1; (b) 0.6 min, (c) 4.6 min and (d) 19.5 min after $^{t}$BuOOH addition.

EPR, Mössbauer, EXAFS and XANES techniques. Complexes **3** and **4** were prepared by the treatment of **1** with 7.2 equivalents of BuOOH in $CH_2Cl_2$ and $CH_2Br_2$, respectively, with 95 and 94% yields.

## EPR and Mössbauer data

The EPR spectrum of solid **1** showed a wide isotropic signal with g = 2.091 without hyperfine structure, probably because of exchange broadening effects. The formation of **3** and **4** led to the disappearance of iron signals and the appearance of a symmetric strong and narrow signal (11 G width) at g = 2.0012 (Fig. 4), which is typical for organic radicals. A similar EPR signal was observed for the phthalocyanine cation radical obtained by electrochemical oxidation of LiPc.[13]

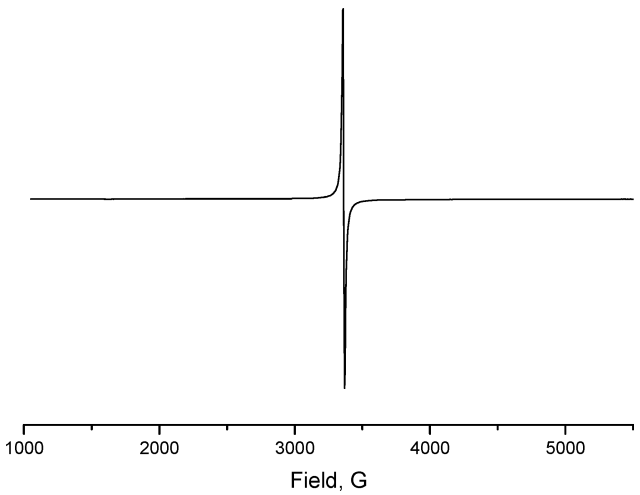


**Fig. 4** Solid state EPR spectrum of complex **3** at 77 K.

The zero-field Mössbauer spectrum of solid **3** exhibited one doublet with $\delta = -0.10$ mm s$^{-1}$ and quadrapolar splitting $\Delta E_Q =$ 1.64 mm s$^{-1}$, indicating identical Fe(IV) sites (Fig. 5).[7,14] Thus, EPR and Mössbauer data are in agreement about the EPR silent Fe(IV)Fe(IV) structure and the presence of the cation radical on one phthalocyanine ligand.

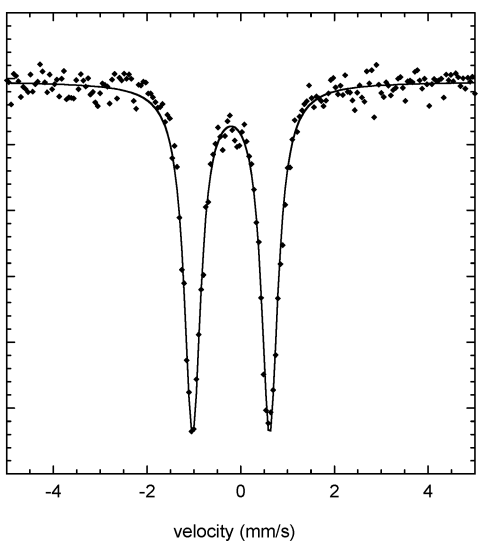


**Fig. 5** Mössbauer spectrum of compound **3** recorded at 77 K. Calculated parameters from the spectrum: $\delta = -0.10$ mm s$^{-1}$, $\Delta E_Q = 1.64$ mm s$^{-1}$, line width $W = 0.22$ mm s$^{-1}$, relative spectral area: 100%.

### Fe K-edge extended X-ray absorption fine structure (EXAFS)

According to the molecular dynamics optimisation, the iron atoms in **1** are moved slightly out of the Pc plane. They are "pulled" into the interlayer space by the axial Fe–N bonds. Simple molecular mechanics (MM+) simulations suggest that addition of halogen atoms leads to the expected symmetrization of the environment of iron, with its return into the Pc plane. These models were used as a starting point for further interpretation and fitting of X-ray absorption spectroscopy (XAS) experimental data. The experimental results of the EXAFS measurements are presented in the Fourier transform (FT) form in Fig. 6.

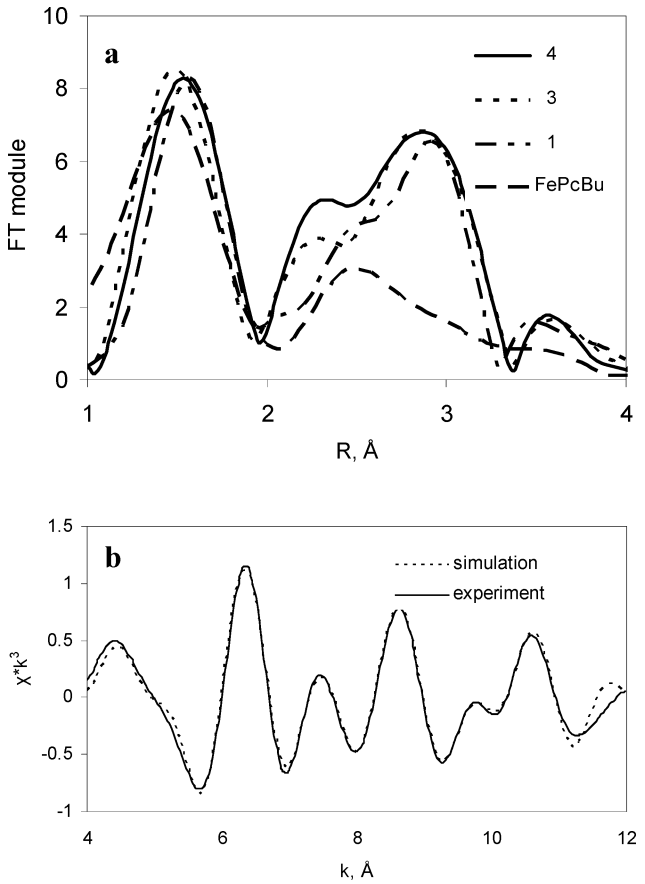


**Fig. 6** EXAFS FT spectra of mononuclear $Fe^{III}(OH)Pc^{t}Bu$ and complexes **1**, **3** and **4** (a); and K-space EXAFS fitting of complex **4** (b). FePcBu stands for mononuclear $Fe^{III}(OH)Pc^{t}Bu$. Due to the phase shift, the distances on the graph are lower than the fitted values.

Strictly speaking, the FT curves of multi-shell EXAFS signals cannot be described as the superposition of the signals from the corresponding shells, but must be treated as a result of their complex interference. However, for the shells of neighbours with distances differing by more than 0.5 Å, the total FT curve can be approximately considered as consisting of independent peaks, where each peak corresponds to a separate shell or to a group of shells. From this point of view, the FT spectra presented in Fig. 6 can be qualitatively discussed as being composed by contributions of different "groups". The first low distance lump is due to the first nitrogen neighbour from four coordinating in-plane nitrogen atoms at *ca.* 1.9 Å and from the bridging N atom at *ca.* 1.6 Å. Note that the intensity from the bridging N atom does not add to the main signal from the phthalocyanine nitrogens but negatively interfere with it, leading to the shift of the whole maximum to higher distances. The second group contains contributions from the non-coordinating light atoms of the ring and for dimeric species, contributions from the iron atoms bridged by Fe–N–Fe bond, as well as to the closest light atoms from the other phthalocyanine ring. Due to the presence of the second phthalocyanine entity, the intensity of this second maximum is much higher in the dimer as compared to the monomer.

The peak from the axial nitrogen atom and iron is additionally increased due to the strong contribution of multiple scattering due to the linearity of the Fe–N–Fe fragment. Adding halogens does not change the shape of this maximum. Therefore, it can be supposed that the dimeric structure is preserved in complexes **3** and **4**. At the same time, an intense shoulder appears in the halogen adducts, which is expectedly stronger in **4** than in **3** and which is shifted to the right, because of the higher atomic mass of bromine and the longer Fe–Br distance compared to Fe–Cl.

The fitting of the curves with seven and eight shell models for complex **1** and halogen derivatives **3** and **4** proves the qualitative conclusions made above: the dimer structure is not destroyed but somewhat relaxed due to the halogen atom addition. One atom of halogen is bonded to Fe scatterer. The values of the parameters for the initial **1** and complex **4** are listed in the Table 1. For Cl-containing complex **3**, the results are essentially the same but the Fe–Cl distance was 2.33 Å.

### X-Ray absorption near-edge structures (XANES)

The shape and position of the pre-edge peak and of the main jump in the XANES spectra depend on the oxidation state and

**Table 1** Results of the EXAFS fitting for the Fe K edge spectra of **1**, **3** and **4**

| Scatterer atom | *R*/Å | Number | Debye–Waller (DW) factor/Å$^2$ | $\Delta E_0$ |
|---|---|---|---|---|
| Complex **1** | | | | |
| N | 1.94(1) | 4 | 0.0039(6) | –4.7(5) |
| N | 1.65 (1) | 1 | 0.0039(6) | –2.3(5) |
| N | 3.41(2) | 4 | 0.0030(8) | –2.3(5) |
| Fe | 3.33(1) | 1 | 0.0020(8) | –1.1(5) |
| C | 3.07(2) | 8 | 0.0040(8) | –2.0(5) |
| N | 4.06(1) | 4 | 0.0030(8) | –2.3(5) |
| C | 4.26(2) | 8 | 0.0070(8) | — |
| Complex **3** | | | | |
| N | 1.94(1) | 4 | 0.0035(5) | -4.5(5) |
| N | 1.68(1) | 1 | 0.0037(5) | -5.0(5) |
| N | 3.42(2) | 4 | 0.0038(8) | -3.0(5) |
| Fe | 3.35(2) | 1 | 0.0020(8) | -3.8(5) |
| C | 3.07(2) | 8 | 0.0043(8) | -3.0(5) |
| N | 4.07(3) | 4 | 0.004(1) | -4(1) |
| C | 4.24(4) | 8 | 0.007(1) | -4(1) |
| Cl | 2.33(3) | 1.1(2) | 0.009(1) | -5(1) |
| Complex **4** | | | | |
| N | 1.93(1) | 4 | 0.0035(6) | -5.0(5) |
| N | 1.69(1) | 1 | 0.0035(6) | -4.0(5) |
| N | 3.45(2) | 4 | 0.0030(6) | -5.0(5) |
| Fe | 3.39(1) | 1 | 0.0020(8) | -3.7(5) |
| C | 3.08(2) | 8 | 0.0044(8) | -2.5(5) |
| N | 4.07(2) | 4 | 0.0030(8) | -4(1) |
| C | 4.25(2) | 8 | 0.007(1) | -3.8(8) |
| Br | 2.54(4) | 0.9(2) | 0.008(1) | -7(2) |

geometry of the iron scatterer. The pre-edge region is more characteristic and sensitive to the variation of the oxidation state and coordination of the Fe atom. The pre-edge parts of the spectra of initial complex **1** and dihalogen derivatives **3** and **4** are presented in Fig. 7a, together with a mononuclear $Fe^{III}(OH)Pc^{t}Bu$ reference.

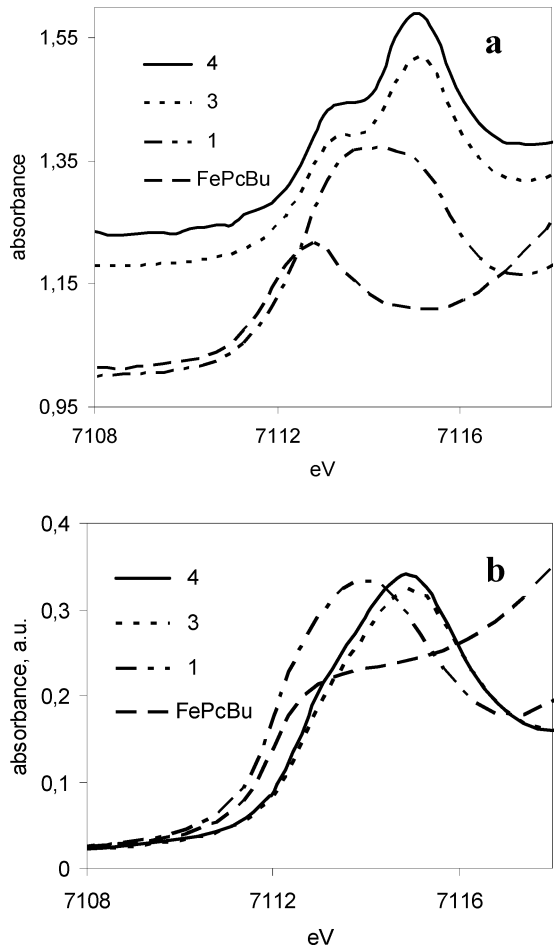


**Fig. 7** Pre-edge parts of the XAS spectra of mononuclear $Fe^{III}(OH)Pc^{t}Bu$, dimeric **1**, **3** and **4**: (a) experimental curves; (b) FEFF simulations. FePcBu stands for mononuclear $Fe^{III}(OH)Pc^{t}Bu$.

The XANES spectrum of monomeric $FePc^{t}Bu$ has a small pre-edge peak at 7112.8 eV, typical for the octahedral or square-pyramidal Fe(III) complexes.[15] The pre-edge transition is assigned to a dipole-forbidden but quadrupole-allowed 1s→3d transition. The rising part of curve at higher energy corresponds to the 1s–4p Fe orbital transition.[16]

Formation of nitrido dimer **1** resulted in the increase of pre-edge intensity and shift of the pre-edge peak to a higher energy of 7114.1 eV. The increase of the pre-edge intensity is consistent with oxidation of iron since it increases the number of free d-orbitals and therefore the probability of the 1s–3d electron transfer. The blue shift of the pre-edge is also consistent with the oxidation as it results in the increase of the efficient positive charge on the iron central ion and therefore stronger electron bonding. These relationships between the iron pre-edge position and oxidation state were reported earlier.[17]

In the halogen adducts **3** and **4**, further increase of pre-edge energy occurs (7115.2 eV for both **3** and **4**) and the second lobe of the pre-edge peak appears at 7113.4 eV, as clearly seen from the experimental spectra (Fig. 7a). The increase of pre-edge energy reflects the higher oxidation state of iron with respect to that of **1**. The existence of two lobes in complexes **3** and **4** can probably be explained by the non-equivalent character of Fe sites because of the presence of the cation radical on one phthalocyanine ligand. It could lead to the removal of 3d orbital degeneration and the occurrence of multiple excited states, resulting in the superposition of two types of pre-edges. It should be noted that while the systematic error of pre-edge peak position and Fermi energy for the light transition elements may be about 1 eV, for the sequences of similar compounds, the FEFF8 simulations provide a much better precision of about 0.2 eV.

In summary, EXAFS fitting and FEFF simulation of the XANES region corroborate the formation of complexes **3** and **4** without perturbing the μ-nitrido dimeric structure. As found both by EXAFS analysis and FEFF simulations for halogen adducts **3** and **4**, the optimal iron–halogen distance in both compounds corresponds to the formation of Fe–Br and Fe–Cl covalent bonds (2.54 and 2.33 Å, respectively).

### Structure of complexes 3 and 4

On the basis of spectroscopic data, we propose a tentative reaction scheme for the formation of **2**, **3** and **4**, as well as their formulations (Scheme 1).

In the first step, **1** coordinates $^{t}BuOOH$ to form the peroxo complex $Fe^{IV}NFe^{III}OO^{t}Bu$, detectable by ESI-MS. The peroxo complex can undergo homolytic or heterolytic cleavage of the O–O bond to form powerful oxidizing species.[3] The mechanism of the oxidation of $CH_2X_2$ (X = Cl, Br) by this species to provide X for complexes **2–4** is not yet clear. The first rapidly formed intermediate, **2**, contains one halogen atom and cation radical on the phthalocyanine ligand, as indicated by ESI-MS and UV-vis data, respectively. Its further oxidation affords Fe(IV) dihalogen complexes **3** and **4**. Mössbauer, EPR and XANES data are consistent with the Fe(IV)Fe(IV) formulation of dimers **3** and **4**. EXAFS data indicate hexacoordinated iron atoms situated in the $N_4$ phthalocyanine plane. Pentacoordinated iron centers are typically displaced out of macrocycle planes.[3d] The increase of the Fe–Fe distance from 3.33 Å in **1** to 3.39 Å in **3** and **4** is also in agreement with the axial coordination of halogen ligands. The Fe–Cl and Fe–Br distances, 2.33 Å and 2.54 Å, respectively, suggest the covalent character of these bonds. Because of the cation radical located at the phthalocyanine ligand (UV-vis, EPR data), **3** and **4** can be considered as having two redox equivalents of a higher oxidation state than in **1**.

Complexes **3** and **4** seem to be very stable at ambient conditions, at least for several months. This is a rare case of stable Fe(IV) complexes. Nevertheless, taking into account the high oxidation state of Fe and the presence of the cation radical on the phthalocyanine ligand, one can expect that **3** and **4** will show some oxidizing activity. In order to check this proposal and to confirm the formulation of **3** and **4**, we studied the stoichiometry of oxidation of thiols to disulfides (one electron oxidation) and hydroquinone to quinone (two electron oxidation).

 

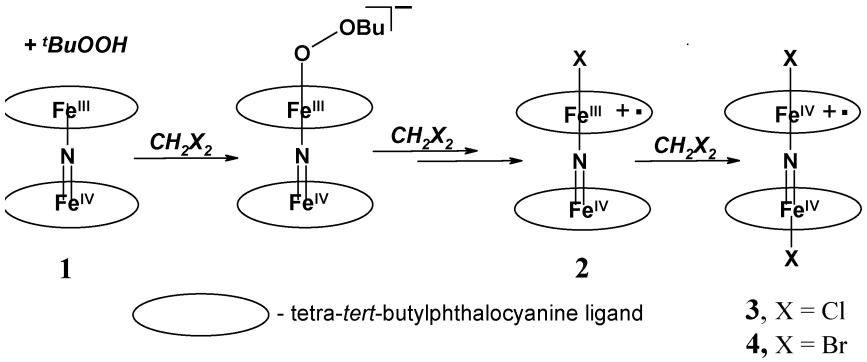


**Scheme 1** Structures of the complexes obtained from **1** and $^{t}$BuOOH in $CH_2X_2$ (X = Cl, Br)

### Titration of 3 with reductants

We found that complexes **3** and **4** can be reduced in the presence of one and two electron reductants. The titration of **3** with 2-mercaptoethanol showed that 2 equivalents of the substrate were oxidized by 1 equivalent of **3**, with regeneration of initial **1** (Fig. 8, 9).

The UV-vis spectra of this titration exhibited very clean isosbestic points (Fig. 8). Disulfide was detected by GC-MS as the only reaction product. In turn, when hydroquinone was used as a substrate, 1 equivalent of **3** was consumed for the oxidation of 1 equivalent of hydroquinone to the corresponding quinone. These data provide evidence that **3** and **4** have two redox equivalents above the oxidation state of **1**, which is compatible with the formulation of these species as (Cl)PcFe$^{IV}$–N–Fe$^{IV}$Pc$^{+\bullet}$(Cl) and (Br)PcFe$^{IV}$–N–Fe$^{IV}$Pc$^{+\bullet}$(Br), respectively.

### Catalytic oxidation of 2-mercaptoethanol

Oxidation of thiols to disulfides is an important biological and industrial process.[18] Cobalt and iron monomeric homogeneous[19] and heterogeneous[20] phthalocyanine catalysts are useful for chemical, photochemical and electrochemical oxidation of thiols. The catalytic activity of metallophthalocyanines in thiol oxidation strongly depends on the pH. The presence of bases is often necessary for high catalytic activity. It is generally accepted that monomeric metallophthalocyanines are active in this reaction and dimerization suppresses the catalytic activity. The catalytic properties of **3** were evaluated in the aerobic oxidation of 0.1 M solutions of 2-mercaptoethanol and 2-mercaptophenol in MeCN at 20 °C. In the presence of 0.1 mol% of **3**, 100% selective conversion of 2-mercaptoethanol to disulfide was observed after 5 h (Fig. 10).

Similarly, 2-mercaptophenol was quantitatively converted to the corresponding disulfide with almost the same oxidation rate. It is worth noting that the addition of a small amount of acid didn't suppress the catalytic activity (as with monomeric metallophthalocyanines) but significantly increased the rate of 2-mercaptoethanol oxidation (Fig. 10). Complete conversion was attained after 1 h. Previously, we have observed the accelerating effect of diluted acid in the oxidation of methane.[3a] Thus, the N-bridged binuclear iron complex showed a high catalytic activity in the aerobic oxidation of thiols under conditions different from those usually used in the presence of mononuclear metallophthalocyanines.

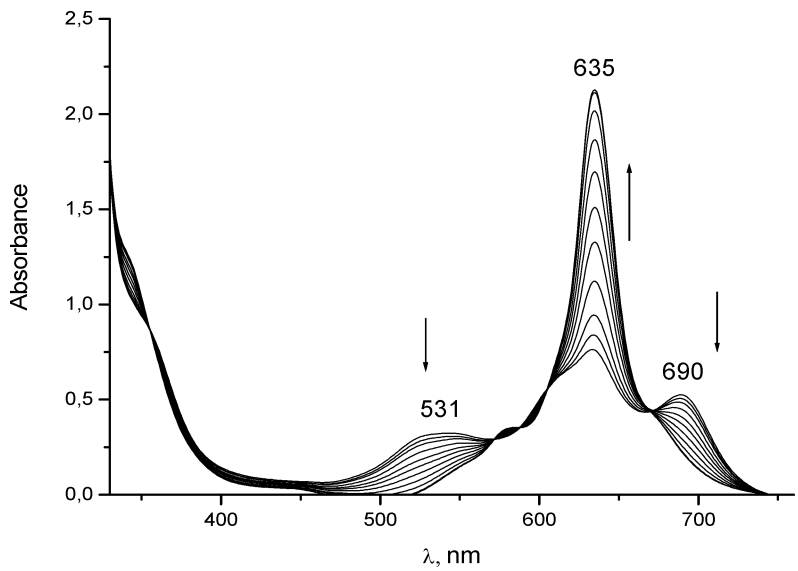


**Fig. 8** Spectral changes during the titration of **3** with 2-mercaptoethanol. [**3**] = $6.9 \times 10^{-6}$ M, 25 °C, acetonitrile.

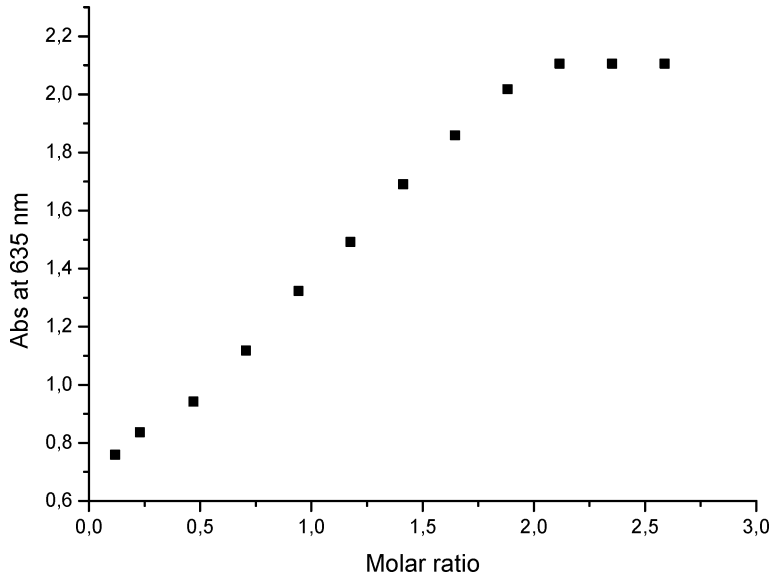


**Fig. 9** Dependence of absorbance at 635 nm on the molar ratio of **3** *vs.* 2-mercaptoethanol.

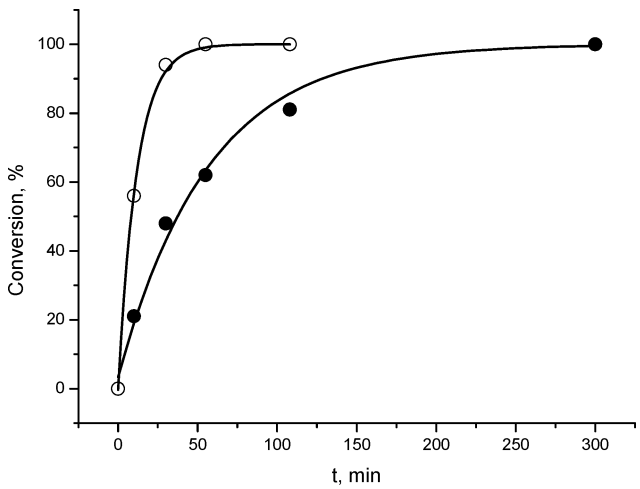


**Fig. 10** Catalytic oxidation of 2-mercaptoethanol by complex **3** in MeCN solution (●) and in 1% of $H_2SO_4$ in MeCN (○).

## Conclusions

N-bridged diiron complex **1** in combination with $^t$BuOOH exhibits a rare reactivity. It is capable of dechlorinating $CH_2Cl_2$ and debrominating $CH_2Br_2$ to form binuclear N-bridged hexacoordinated X-(Pc)$Fe^{IV}NFe^{IV}$($Pc^{+\bullet}$)-X complexes with two Fe–Cl and Fe–Br bonds, respectively. This finding represents a novel method of the preparation of these unusual complexes. High valent mono- and binuclear iron (IV) complexes bearing a cation radical on a macrocyclic ligand relevant to biological and biomimetic oxidations are usually unstable elusive species. Two N-bridged diiron(IV) phthalocyanine cation radical complexes, **3** and **4**, prepared in this work represent a rare case of stable complexes which can be easily characterized to provide valuable spectroscopic data. These data can be useful for the analysis of similar but unstable species involved in the oxidation.[3] Complex **3** showed a promising catalytic activity in single turnover and catalytic oxidation of thiols and hydroquinone. This is the first example of the application of the X-(Pc)$Fe^{IV}NFe^{IV}$($Pc^{+\bullet}$)-X complex as a catalyst.

Although further work is still required to understand the mechanisms involved in the formation of N-bridged diiron phthalocyanine cation radical complexes with halogen axial ligands, the present results confirm the potential of the Fe–N–Fe platform in oxidation catalysis.

## Experimental

### General methods

UV-Vis spectra of solutions and kinetic traces were recorded on a Perkin-Elmer Lambda 35 spectrophotometer. UV-Vis measurements were performed in MeCN (HPLC grade) at 25 °C. X-Band (9.5 GHz) EPR spectra were recorded at 77 K on a Bruker ESP 300E spectrometer using a standard rectangular (TE102) EPR cavity (Bruker ER4102ST). Microwave power of 1.6 mW and a modulation amplitude of 1 G was used. For quantitative analysis, the EPR spectra were simulated and the experimental spectra were fitted using the simulation program EasySpin.[21] A two stage fitting was implemented, beginning with Nelder/Mead downhill simplex with coarse termination criteria and followed by refinement using Levenberg/Marquardt iterative algorithm. XAS experiments were carried out at the BM01 beam line of the ESRF synchrotron facility, Grenoble. The Fe K-edge spectra were monitored in transmission mode, using a Si(111) crystal monochromator. The data were treated with FEFF (amplitudes and phases calculation)[22] and VIPER (fitting)[23] programs. The edge background was extracted using Bayesian smoothing with a variable number of knots. The curve fitting was done alternatively in the $R$ and $k$ spaces, and the fit was accepted in the case of simultaneous convergence in $k$ and $R$ spaces. Coordination numbers (CN) were fixed and equal to the values from the supposed molecular structure, except halogen atoms, for which the CNs was freely fitted. Interatomic distances ($R$), the Debye–Waller parameter ($\sigma^2$), and energy shifts ($\Delta E_0$) were used as fitting

 

variables. True Debye–Waller (DW) factors and amplitude factors were decorrelated from the coordination numbers by the fitting of spectra multiplied by different powers of $k$, similar to the treatment of spectra in a previous work.[24] Constraints were introduced on the variables, such as DW factors or energy shifts, to get values that lie in physically reasonable intervals. Constraints imposed by the molecular structure were also introduced. Real space full multiple scattering *ab initio* FEFF8.2 code was applied to simulate XANES spectra and pre-edge peaks, with the FMS and SCF radii between 4 and 5 Å, *i.e.* including the whole phthalocyanine ligand that coordinates the scatterer and the closest iron, nitrogen and carbon atoms from the second phthalocyanine plane of $(FePc^{t}Bu_4)_2N$. In order to simulate the spectra of **3** and **4**, which have never been prepared in the crystalline form, the initial guess of the structure was made on the basis of a known structure similar to **4**. Then, the molecular geometry was optimized using molecular dynamics (MM+ field force). After that, the nearest and second neighbour cluster of 35 atoms were extracted from this optimized structure to carry out further simulations. Note that simulations using the full molecule set proved to be time consuming without being more accurate. The XYZ Cartesian coordinates of this cluster were then plugged into the FEFF input files. For the non-symmetric adducts, the simulated XANES spectra were obtained from the averaging of the model spectra, with a hole on the different iron atoms. We checked this point, performing several simulations with the full molecular set, and found no significant differences compared to the abridged two-shell cluster. Full multiple scattering and self consistent field calculation radii were set to 4 Å.

The reaction products were identified by GC-MS (Hewlett Packard 5973/6890 system; electron impact ionization at 70 eV, He carrier gas, 30 m × 0.25 mm cross-linked (5%-phenyl)-methylpolysiloxane (0.25 μm coating) capillary column, HP-5MS. The quantitative analysis of reaction mixtures was performed the using GC (Agilent 4890D system; 30 m × 0.52 mm chrompack capillary column CP-Sil 8 cp).

### Materials

Tetra-*tert*-butylphthalocyaninatoiron[25] and μ-nitrido-bis[tetra-(*tert*-butyl)phthalocyaninatoiron][3a] (**1**) were prepared as previously described.

**μ-Nitrido-bis[tetra(*tert*-butyl)phthalocyaninatoiron] dichloride (3).** μ-Nitrido-bis[tetra(*tert*-butyl)phthalocyaninatoiron] (**1**, 160 mg, 0.1 mmol) was dissolved in 20 ml of dichloromethane and 100 μl of 70% tBuOOH (0.723 mmol) was added to the solution. The mixture was refluxed for 6 h, then solvent and excess oxidant were evaporated under reduced pressure at 25 °C. Yield: 160 mg, 95%. ESI-MS: 1670.5 [$M^+$]; calculated for $C_{96}H_{96}N_{17}Fe_2Cl_2$: 1670.6; UV-vis ($CH_3CN$): $\lambda_{max}$ (log $\varepsilon$) 340 (5.40), 547 (4.83), 636 (5.21), 691 (5.09) nm; IR (KBr): $\nu$ = 3061 (C–$H_{ar}$), 2951 (C–$H_{alk}$), 1615 (C=N), 1483 (C=C), 1393, 1364 (δ $(CH)_{tBu}$), 1350 (Pc cation radical), 1324, 1310, 1280, 1256, 1200, 1089, 1050, 935 (Fe = N), 894, 833, 754, 693, 671 $cm^{-1}$.

**μ-Nitrido-bis[tetra(*tert*-butyl)phthalocyaninatoiron] dibromide (4).** μ-Nitrido-bis[tetra(*tert*-butyl)phthalocyaninatoiron] (**1**, 80 mg, 0.05 mmol) was dissolved in 20 ml of dibromomethane and 50 μl of 70% tBuOOH (0.362 mmol) was added to the solution, which was then stirred for 1h. The color of the solution changed from greenish-blue to deep blue. The solvent and the excess of the oxidant were removed. The solid was washed with water and dried. Yield: 83 mg, 94%. UV-Vis ($CH_3CN$): $\lambda_{max}$ (rel. intensity) 339 (1.0), 550 (0.29), 637 (0.64), 695 (0.41) nm; IR (KBr): $\nu$ = 3063, 2963, 2868, 1617, 1482, 1456, 1364, 1326, 1311, 1292, 1258, 1200, 1092, 1056, 1020, 940, 834, 754, 694, 649 $cm^{-1}$.

**Interaction of 3 with hydroquinone.** Hydroquinone (11.0 mg, 0.1 mmol) was dissolved in 5 ml of deoxygenated acetonitrile (0.02 M solution) containing 0.05 M chlorobenzene as internal standard. Complex **3** (33.4 mg, 0.02 mmol) was added to the solution. The resulting mixture was stirred for 20 min and analyzed by GC. Conversion of hydroquinone and selectivity in quinone were 18% and 92%, respectively.

**Interaction of 3 with 2-mercaptoethanol.** Aliquots of deoxygenated $10^{-3}$ M or $10^{-4}$ M solutions of $HSCH_2CH_2OH$ in MeCN were added to a deoxygenated $6.9 \times 10^{-6}$ M solution of complex **3** in MeCN. The UV-vis spectra were recorded 10 min after addition of the substrate.

**Catalytic oxidation of 2-mercaptoethanol and 2-mercaptophenol.** A 50 mL flask was charged with 2 mL of acetonitrile, containing $10^{-4}$ M catalyst, **3**, and 0.1 M substrate. The products were identified by GC-MS. The course of the reaction was monitored by GC using chlorobenzene as internal standard.

## Acknowledgements

This work was supported by grant ANR-08-BLAN-0183-01 from Agence Nationale de la Recherche (ANR, France). We thank the European Synchrotron Radiation Facility (ESRF, Grenoble) for the provision of synchrotron radiation facilities and Dr O. Safonova for assistance in using beam line BM01.

## Notes and references

1 (*a*) M.-H. Baik, M. Newcomb, R. A. Rriesner and S. J. Lippard, *Chem. Rev.*, 2003, **103**, 2385–2419; (*b*) L. J. Murray and S. J. Lippard, *Acc. Chem. Res.*, 2007, **40**, 466–474; (*c*) E. G. Kovaleva, M. B. Neibergall, S. Chakrabarty and J. D. Lipscomb, *Acc. Chem. Res.*, 2007, **40**, 475–483.
2 (*a*) E.Y. Tshuva and S. J. Lippard, *Chem. Rev.*, 2004, **104**, 987; (*b*) L. Que, Jr. and W. B. Tolman, *Nature*, 2008, **455**, 333–340; (*c*) A. A. Shteinman, *Russ. Chem. Rev.*, 2008, **77**, 945–966.
3 (*a*) A. B. Sorokin, E. V. Kudrik and D. Bouchu, *Chem. Commun.*, 2008, 2562–2564; (*b*) E. V. Kudrik and A. B. Sorokin, *Chem.–Eur. J.*, 2008, **14**, 7123–7126; (*c*) E. V. Kudrik, P. Afanasiev, D. Bouchu, J. M. M. Millet and A. B. Sorokin, *J. Porphyrins Phthalocyanines*, 2008, **12**, 1078–1079; (*d*) Ü. İşci, P. Afanasiev, M. M. Millet, E. V. Kudrik, V. Ahsen and A. B. Sorokin, *Dalton Trans.*, 2009, 7410–7420.
4 (*a*) L. A. Bottomley, J.-N. Gorce, V. L. Goedken and C. Ercolani, *Inorg. Chem.*, 1985, **24**, 3733–3737; (*b*) C. Ercolani, M. Gardini, G. Pennesi, G. Rossi and U. Russo, *Inorg. Chem.*, 1988, **27**, 422–424; (*c*) B. J. Kennedy, K. S. Murray, H. Homborg and W. Kalz, *Inorg. Chim. Acta*, 1987, **134**, 19–21.
5 (*a*) D. A. Summerville and I. A. Cohen, *J. Am. Chem. Soc.*, 1976, **98**, 1747–1752; (*b*) W. R. Scheidt, D. A. Summerville and I. A. Cohen, *J. Am. Chem. Soc.*, 1976, **98**, 6623–6628; (*c*) K. M. Kadish, L. A. Bottomley, J. G. Brace and N. Winograd, *J. Am. Chem. Soc.*, 1980, **102**, 4341–4344; (*d*) G. A. Schick and D. F. Bocian, *J. Am. Chem. Soc.*, 1983, **105**, 1830–1838; (*e*) D. F. Bocian, E. W. Findsen, J. A. Hofmann, Jr., G. A. Schick, D. R. English, D. N. Hendrickson and K. S. Suslick, *Inorg. Chem.*, 1984, **23**, 800–807; (*f*) D. R. English, D. N. Hendrickson and K. S. Suslick, *Inorg. Chem.*, 1985, **24**, 121–122; (*g*) M. Li, M. Shang, N. Ehlinger, C. E. Schulz and W. R. Scheidt, *Inorg. Chem.*, 2000, **39**, 580–583.

6 (*a*) C. Ercolani, S. Hewage, R. Heucher and G. Rossi, *Inorg. Chem.*, 1993, **32**, 2975–2977; (*b*) C. Ercolani, J. Jubb, G. Pennesi, U. Russo and G. Trigiante, *Inorg. Chem.*, 1995, **34**, 2535–2541; (*c*) M. P. Donzello, C. Ercolani, K. M. Kadish, Z. Ou and U. Russo, *Inorg. Chem.*, 1998, **37**, 3682–3688; (*d*) M. P. Donzello, C. Ercolani, U. Russo, A. Chiesi-Villa and C. Rizzoli, *Inorg. Chem.*, 2001, **40**, 2963–2976; (*e*) P. A. Stuzhin, M. Hamdush and H. Homborg, *Mendeleev Commun.*, 1997, **7**, 196–198; (*f*) K. Meyer, E. Bill, B. Mienert, T. Weyhermüller and K. Wieghardt, *J. Am. Chem. Soc.*, 1999, **121**, 4859–4876; (*g*) T. Jüstel, M. Müller, T. Weyhermüller, C. Kressl, E. Bill, P. Hildebrandt, M. Lenglen, M. Grodzicki, A. X. Trautwein, B. Nuber and K. Wieghardt, *Chem.–Eur. J.*, 1999, **5**, 793–810; (*h*) T. Jüstel, T. Weyhermüller, K. Wieghardt, E. Bill, M. Lenglen, A. X. Trautwein and P. Hildebrandt, *Angew. Chem., Int. Ed. Engl.*, 1995, **34**, 669–672; (*i*) P. A. Stuzhin, L. Latos-Grażyński and A. Jezierski, *Transition Met. Chem.*, 1989, **14**, 341–346.

7 B. Floris, M. P. Donzello, and C. Ercolani, in *Porphyrin Handbook*, ed. K. M. Kadish, K. M. Smith and R. Guilard, Elsevier Science, San Diego, 2003, vol. 18, pp. 1–62.

8 (*a*) W. D. Wagner and K. Nakamoto, *J. Am. Chem. Soc.*, 1988, **110**, 4044–4045; (*b*) W. D. Wagner and K. Nakamoto, *J. Am. Chem. Soc.*, 1989, **111**, 1590–1598; (*c*) T. Petrenko, G. S. DeBeer, N. Aliaga-Alcalde, E. Bill, B. Mienert, Y. Xiao, Y. Guo, W. Sturhahn, S. P. Cramer, K. Wieghardt and F. Neese, *J. Am. Chem. Soc.*, 2007, **129**, 11053–11060.

9 J. F. Berry, E. Bill, E. Bothe, S. D. George, B. Mienert, F. Neese and K. Wieghardt, *Science*, 2006, **312**, 1937–1941.

10 (*a*) D. R. English, D. N. Hendrickson and K. S. Suslick, *Inorg. Chem.*, 1983, **22**, 367–368; (*b*) M. Li, M. Shang, N. Ehlinger, C. E. Schulz and W. R. Scheidt, *Inorg. Chem.*, 2000, **39**, 580–583; (*c*) E. N. Bakshi, C. D. Delfs, K. S. Murray, B. Peters and H. Homborg, *Inorg. Chem.*, 1988, **27**, 4318–4320.

11 B. P. Moubaraki, D. Benlian, A. Baldy and A. Pierrot, *Acta Crystallogr., Sect. C: Cryst. Struct. Commun.*, 1989, **45**, 393–394.

12 (*a*) E. Ough, Z. Gasyna and M. J. Stillman, *Inorg. Chem.*, 1991, **30**, 2301–2310; (*b*) T. Nyokong, Z. Gasyna and M. J. Stillman, *Inorg. Chem.*, 1987, **26**, 548–553.

13 P. Turek, J. J. André, A. Girardeau and J. Simon, *Chem. Phys. Lett.*, 1987, **134**, 471–476.

14 (*a*) M. Hanack, U. Keppeler, A. Lange, A. Hirsch and R. Dieing, in *Phthalocyanines: Properties and Applications*, ed. C. C. Leznoff and A. B. P. Lever, VCH, New York, 1993, vol. 2, pp. 46–96; (*b*) V. N. Nemykin, A. E. Polshina, V. Y. Chernyi, E. V. Polshin and N. Kobayashi, *J. Chem. Soc., Dalton Trans.*, 2000, 1019–1025.

15 C. Cartier, M. Momenteau, E. Dartyge, A. Fontaine, G. Tourillon, A. Michalowicz and M. Verdaguer, *J. Chem. Soc., Dalton Trans.*, 1992, 609–618.

16 S. Y. Ha, J. Park, T. Ohta, G. Kwag and S. Kim, *Electrochem. Solid-State Lett.*, 1999, **2**, 461–464.

17 G. A. Waychunas, M. J. Apted and G. E. Brown, *Phys. Chem. Miner.*, 1983, **10**, 1–9.

18 B. Basu, S. Satapathy and A. K. Bhatnagar, *Catal. Rev. Sci. Eng.*, 1993, **35**, 571–609.

19 (*a*) H. Shirai, H. Tsuiki, E. Masuda, T. Koyama, K. Hanabusa and N. Kobayashi, *J. Phys. Chem.*, 1991, **95**, 417–423; (*b*) V. Iliev and A. Mihaylova, *J. Photochem. Photobiol., A*, 2002, **149**, 23–30; (*c*) S. M. S. Chauhan, A. Kumar and K. A. Srinivas, *Chem. Commun.*, 2003, 2348–2349.

20 (*a*) T. Buck, D. Wöhrle, G. Schulz-Ekloff and A. Andreev, *J. Mol. Catal.*, 1991, **70**, 259–268; (*b*) D. Wöhrle, *Macromol. Rapid Commun.*, 2001, **22**, 68–97; (*c*) D. Wöhrle, O. Suvorova, R. Gerdes, O. Bartels, L. Lapok, N. Baziakina, S. Makarov and A. Slodek, *J. Porphyrins Phthalocyanines*, 2004, **8**, 1020–1041; (*d*) F. Bedioui, S. Griveau, T. Nyokong, J. A. Appleby, C. A. Caro, M. Gulppi, G. Ochoa and J. H. Zagal, *Phys. Chem. Chem. Phys.*, 2007, **9**, 3383–3396.

21 S. Stoll and A. Schweiger, *J. Magn. Reson.*, 2006, **178**, 42–55.

22 A. L. Ankudinov, C. E. Bouldin, J. J. Rehr, J. Sims and H. Hung, *Phys. Rev. B: Condens. Matter Mater. Phys.*, 2002, **65**, 104107.

23 K. V. Klementev, *J. Synchrotron Radiat.*, 2001, **8**, 270–272.

24 D. Genuit, P. Afanasiev and M. Vrinat, *J. Catal.*, 2005, **235**, 302–317.

25 J. Metz, O. Schneider and M. Hanack, *Inorg. Chem.*, 1984, **23**, 1065–1071.

 